J Electroceram (2006) 17:387–391
DOI 10.1007/s10832-006-9637-2

Structure and dielectric properties of $BaTi_4O_9$ thin films for RF-MIM capacitor applications

**Bo-Yun Jang · Beom-Jong Kim · Young-Hun Jeong ·
Sahn Nahm · Ho-Jung Sun · Hwack-Ju Lee**

Received: 28 June 2005 / Revised: 1 June 2006 / Accepted: 29 June 2006

Abstract $BaTi_4O_9$ thin films were grown on a $Pt/Ti/SiO_2/Si$ substrate using RF magnetron sputtering. A homogeneous $BaTi_4O_9$ crystalline phase developed in the films deposited at 550°C and annealed above 850°C. When the thickness of the film was reduced, the capacitance density and leakage current density increased. Furthermore, the dielectric constant was observed to decrease with decreasing film thickness. The $BaTi_4O_9$ film with a thickness of 62 nm exhibited excellent dielectric and electrical properties, with a capacitance density of 4.612 fF/μm^2 and a dissipation factor of 0.26% at 100 kHz. Similar results were also obtained in the RF frequency range (1–6 GHz). A low leakage current density of 1.0×10^{-9} A/cm^2 was achieved at ±2 V, as well as small voltage and temperature coefficients of capacitance of 40.05 ppm/V^2 and –92.157 ppm/°C, respectively, at 100 kHz.

Keywords $BaTi_4O_9$ · RF · Capacitance density · Leakage current density · Dissipation factor

B.-Y. Jang · B.-J. Kim · Y.-H. Jeong · S. Nahm (✉)
Department of Materials Science and Engineering, Korea University, 1-5 Ka, Anam-Dong, Sungbuk-Ku, Seoul 136-701, Korea
e-mail: snahm@korea.ac.kr

H.-J. Sun
Department of Materials Science and Engineering, Kunsan National University, Miryongdong San 68, Kunsan, Korea

H.-J. Lee
New Materials Evaluation Center, Korea Research Institute of Standards and Science, Daeduk Science Town, Taejon 305-600, Korea

Introduction

Metal-Insulator-Metal (MIM) capacitors are important components in RF Integrated Circuits (ICs). To decrease the size of these capacitors, a large capacitance density and a high quality factor are needed in the RF frequency range. A small leakage current density and low voltage and temperature coefficients (VCCs and TCC, respectively) are also required for the MIM capacitors used in RF ICs. SiO_2 and Si_3N_4 are commonly used for MIM capacitors, but the capacitance densities of these materials are rather low, only about ∼2 fF/μm^2 [1, 2]. Recently, Al_2O_3, Ta_2O_5 and HfO_2 dielectrics, which have a higher dielectric constant (k), have been widely investigated with a view to enhancing the capacitance density of these capacitors [3–10]. Al_2O_3 film has a low leakage current and a high capacitance density of 5 fF/μm^2, but it also has a large VCC (∼2000 ppm/V^2) [3, 4]. Al_2O_3 doped Ta_2O_5 film was reported to have a high capacitance density and a low leakage current, but a low Q-value of approximately 40 [5]. HfO_2 film and HfO_2-Al_2O_3 laminates show a high capacitance density and a low leakage current, but their VCC is high and their dissipation factor has not been studied at high frequency(∼GHz) [6–10]. Therefore, new dielectric materials are needed for the next generation of MIM capacitors destined for RF ICs.

There are various microwave dielectric materials that have a high k, a high Q-value, and good thermal stability in the RF frequency range. Thus, if these materials were grown in the form of a thin film for MIM capacitors, the properties required for RF MIM capacitors could easily be obtained. However, previous works on microwave dielectric materials have focused on bulk ceramics, and few studies have been carried out on thin films. In this work, a thin film of $BaTi_4O_9$ microwave dielectric ceramics was grown and its structure and dielectric/electrical properties were investigated, in order to evaluate its potential use in RF MIM capacitors. $BaTi_4O_9$ ceramics were selected because of their excellent microwave dielectric properties with high k value of 36–38, high Q-value of 3500–5000 at 6–10 GHz and good thermal stability [11–13].

Experimental procedure

The $BaTi_4O_9$ film was grown on a Pt/Ti/SiO_2/Si(100) substrate by RF-magnetron sputtering using a 3 inch-diameter $BaTi_4O_9$ target which was synthesized by the conventional solid state method. The deposition was carried out at 550°C in an oxygen and argon (O_2:Ar = 2:8) atmosphere with a total pressure of 8 A. The sputtering power was 100 W and the deposition time ranged from 20 to 60 min. After the deposition, the thin film was annealed at temperatures ranging from 800°C to 900°C in an O_2 atmosphere by a rapid thermal annealing (RTA) system. The microstructure of the $BaTi_4O_9$ film was analyzed by X-ray diffraction (XRD: Rigaku D/max-RC, Japan) and transmission electron microscopy (TEM:Hitachi H-9000NAR Ibaraki, Japan). For the measurement of the dielectric properties at low frequencies (75–1000 kHz), Pt was deposited on the $BaTi_4O_9$ thin films to form the top electrode of a MIM capacitor using conventional DC sputtering. The capacitance and dissipation factor were measured using a precision LCR meter (Agilent 4285A, USA). The leakage current was measured using a voltage source meter (Keithley 2400, USA). For the measurement of the dielectric properties in the RF frequency range, Al was deposited on the thin film to form the top electrode. The Al-electrode was patterned by photolithography to form a circular patched capacitor structure. The complex reflection coefficient was measured from 0.5 to 6 GHz using a Vector Network Analyzer (HP 8710C, USA). The dielectric constant and dissipation factor were calculated from the reflection coefficients of two circular patched capacitors having different inner diameters but the same outer diameters [14–16].

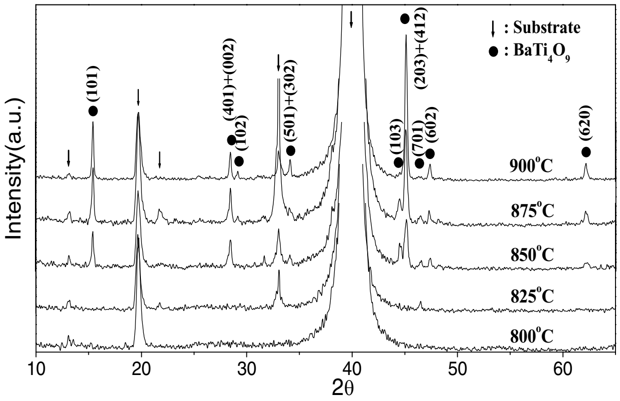

Fig. 1 X-ray diffraction patterns of the $BaTi_4O_9$ films grown at 550°C for 1 h and rapidly thermal annealed at various temperatures for 3 min

Results and discussion

Figure 1 shows the X-ray diffraction patterns of the $BaTi_4O_9$ films grown at 550°C and rapidly thermal annealed at various temperatures. Only the substrate peaks were observed for the samples annealed at temperatures below 850°C. Therefore, an amorphous phase or only a small amount of the $BaTi_4O_9$ crystalline phase was formed for the films grown at 550°C and annealed below 850°C. Peaks for the crystalline phase (indicated by the full circle) appeared for the films annealed at 850°C, and the intensity of these peaks increased with increasing annealing temperature. All the peaks were identified as those of the orthorhombic $BaTi_4O_9$ phase. Therefore, annealing at high temperature (>825°C) is required to obtain the crystallized $BaTi_4O_9$ film.

The microstructure of the $BaTi_4O_9$ film grown at 550°C and annealed at 900°C was investigated using TEM. Figure 2 shows a cross sectional TEM bright field image of this $BaTi_4O_9$ thin film. The inset shows the electron diffraction pattern taken from the same area of the film. The electron diffraction pattern was identified as that of the [200] zone axis of the orthorhombic $BaTi_4O_9$ phase. The thickness of the

Fig. 2 Cross sectional TEM bright field image and the electron diffraction pattern of the $BaTi_4O_9$ thin film

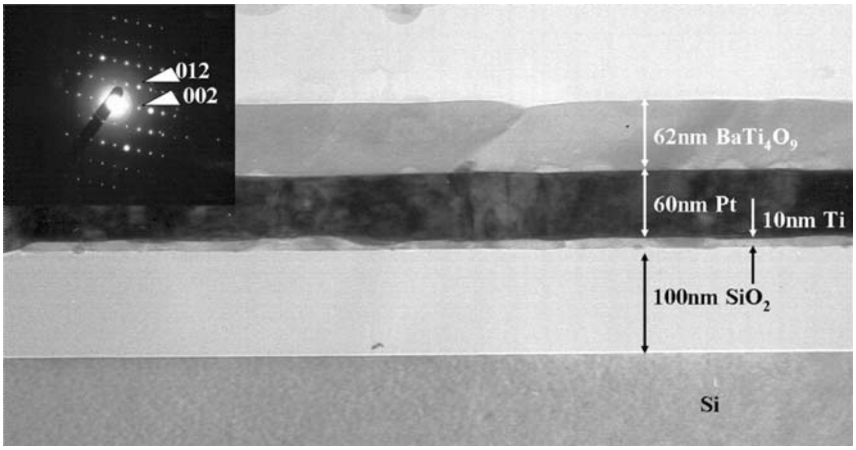

Fig. 3 Capacitance densities and dissipation factors of the $BaTi_4O_9$ films with various thicknesses as a function of frequency

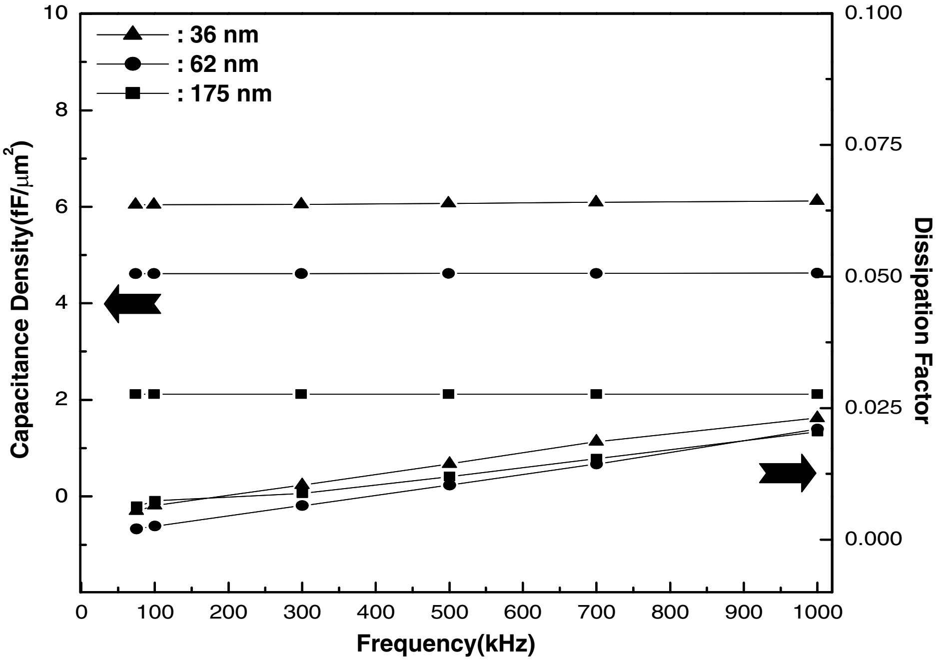

$BaTi_4O_9$ film was 62 nm and a sharp interface was formed between the Pt-bottom electrode and the $BaTi_4O_9$ film. Therefore, it can be concluded that the homogeneous crystalline $BaTi_4O_9$ phase was well developed for the film grown at 550°C and subsequently annealed at 900°C.

The capacitance densities and dissipation factors of $BaTi_4O_9$ films with various thicknesses were measured as a function of the frequency (see Fig. 3). The capacitance density of the $BaTi_4O_9$ film with a thickness of 175 nm was low, being only approximately 2.1 fF/μm^2 and the dielectric constant was about 40, which is similar to that of $BaTi_4O_9$ ceramics. The dissipation factor increased from 0.63% to 2.1% as the frequency was increased from 75 kHz to 1 MHz. The capacitance density increased with decreasing film thickness, and for the $BaTi_4O_9$ film with a thickness of 36 nm, it was about 6.0 fF/μm^2. The dissipation factor increased with decreasing thickness, but this decrease was not significant. The k values for the films with thicknesses of 62 and 36 nm were 32 and 24, respectively. Therefore, it can be concluded that the dielectric constant decreases with decreasing film thickness. In particular, the decrease in the dielectric constant is significant when the thickness of the film is less than 50 nm. However, since the dielectric constant of HfO_2 film with a thickness of 56 nm is about 18, [6] the dielectric constant of the $BaTi_4O_9$ film is comparatively high. According to International Technology Roadmap for Semiconductors (ITRS), a capacitance density of 4.0 fF/μm^2 or higher will be required for the precision analog capacitor from year 2007–2009 [17]. Therefore, the $BaTi_4O_9$ film can easily satisfy the requirements for these analog capacitors provided that the thickness of the film is less than 62 nm.

The capacitance density and dissipation factor of the $BaTi_4O_9$ films were also measured in the 1–6 GHz range, as shown in Fig. 4. For the $BaTi_4O_9$ films with large thicknesses (>60 nm), the capacitance density measured in the RF frequency range was similar to that measured at low frequencies, and the dissipation factor was low. However for the film with a thickness of 36 nm, the capacitance density increased when it was measured at frequencies above 3 GHz. Further studies are needed to understand this increase in the capacitance density, however it is worth mentioning that the $BaTi_4O_9$ film with a thickness of 62 nm exhibits a high capacitance density of 4.1 fF/μm^2 and a low dissipation factor of 0.31% at 2 GHz.

Figure 5 shows the variation in the leakage current density of the $BaTi_4O_9$ films with the applied voltage for various thicknesses. For the 62 nm-thick $BaTi_4O_9$ film, the leakage current density is very low, only 1 nA/cm^2 at ±2 V, which satisfies the ITRS requirement of a leakage current density of 7 fA/pF·V or lower [17]. On the other hand, for the film with a thickness of 36 nm, the leakage current density is too high for the $BaTi_4O_9$ film to be used as an analog capacitor. It is generally accepted that the properties of the interface, especially the oxygen vacancies at the interface, exert the considerable influence on the leakage current of the film. Therefore, the amount of oxygen vacancies at the interface needs to be controlled, in order to reduce the leakage current density of $BaTi_4O_9$ films with thicknesses of less than 50 nm.

The variation in the capacitance with the applied voltage or temperature was measured for 62 nm-thick film which exhibits the high capacitance density and low leakage current density. The VCCs of this film were obtained by using the

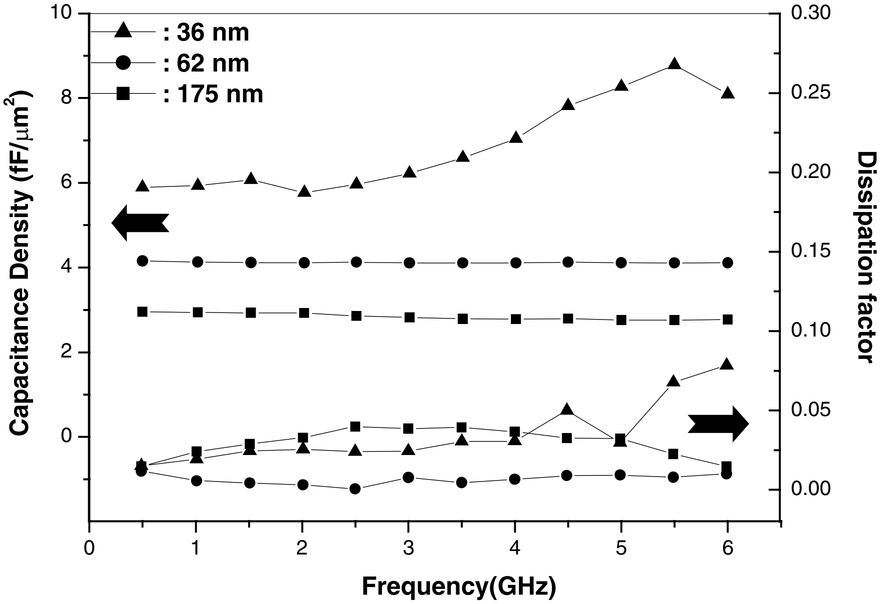

Fig. 4 Capacitance densities and dissipation factors of the $BaTi_4O_9$ films with various thicknesses measured in the RF frequency range

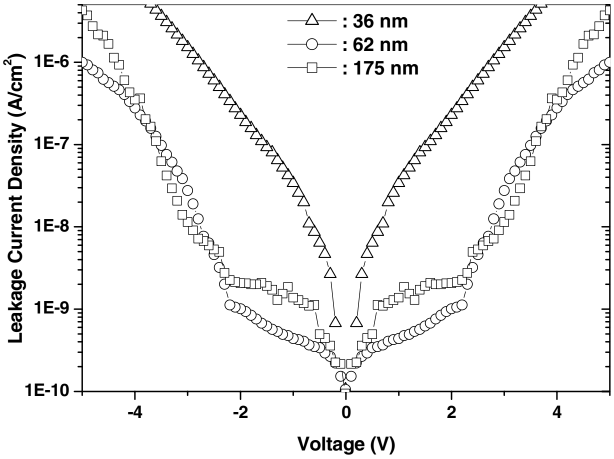

Fig. 5 Leakage current densities of the $BaTi_4O_9$ films with various thicknesses as a function of the applied voltage

second order polynomial equation of the form $C(V)/C_0 = \alpha V^2 + \beta V + 1$, where C_0 is the zero-biased capacitance, and α and β represent the quadratic and linear VCCs, respectively [6]. Figure 6(a) shows the variation of the capacitance density with the applied voltage at 100 and 300 kHz. The VCC values measured at 100 kHz consisted of an α of 40.05 ppm/V^2 and a β of 110.3 ppm/V, which are sufficiently low to meet the requirements ($\alpha < 100$ ppm/V^2, $\beta < 1000$ ppm/V) of RF applications [7, 10]. The TCC values were also measured from 25°C to 100°C at 100 and 300 kHz, as shown in Fig. 6(b). After heating the MIM capacitor up to 100°C, the capacitance was measured at various frequencies during its subsequent cooling. As the temperature decreases, the capacitance density increases, indicating that the $BaTi_4O_9$ film has a negative

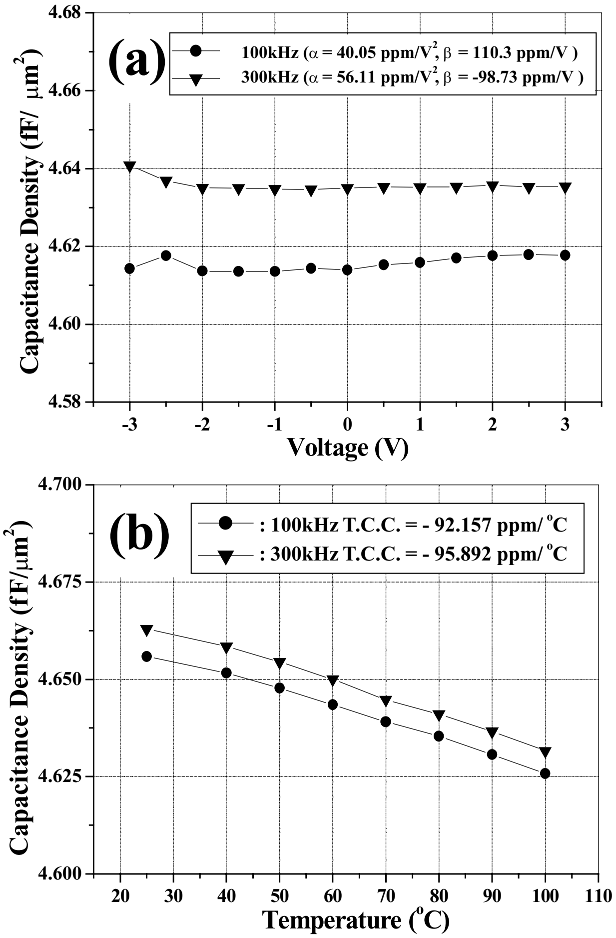

Fig. 6 Variations in the capacitance density of the $BaTi_4O_9$ thin film measured at 100 and 300 kHz as a function of the (a) applied voltage and (b) temperature

TCC. The TCC value of the film measured at 100 kHz is – 92.157 ppm/°C.

Conclusions

$BaTi_4O_9$ thin films were grown on a $Pt/Ti/SiO_2/Si$ substrate using RF magnetron sputtering. The homogeneous $BaTi_4O_9$ crystalline phase was well developed in the film grown at 550°C and subsequently annealed at 900°C. The dielectric and electric properties of $BaTi_4O_9$ film were investigated for the first time, in order to evaluate the possible use in MIM capacitors. A high capacitance density of 4.1 fF/μm^2 was obtained for the $BaTi_4O_9$ film with a thickness of 62 nm. This film also had a low dissipation factor of 0.31% at 2 GHz and a low leakage current density of 1 nA/cm^2 at 2 V. Its VCC and TCC values were also low. Therefore, $BaTi_4O_9$ film is a good candidate material for RF MIM capacitors.

Acknowledgements This work was supported by the Ministry of Science and Technology through the Nano-Technology project and one of the authors also acknowledges the financial support provided by the Ministry of Science and Technology through the NRL project.

References

1. J.A. Babcock, S.G. laster, A. Pinto, C. Dirnecker, P. Steinmann, R. Jumpertz, and B. El-Kareh, *IEEE Elec. Dev. Lett.*, **22**, 230 (2001).
2. A. Farcy, J. Torres, V. Arnal, M. Fayolle, H. Feldis, F. Jourdan, M. Assous, J.L. Di Maria, V. Vidal, *Microelec. Eng.*, **70**, 368 (2003).
3. S.B. Chen, C.H. Lai, A. Chin, J.C. Hsieh, and J. Liu, *IEEE MTT-S Digest*, 201 (2002).
4. S.B. Chen, C.H. Lai, A. Chin, J.C. Hsieh, and J. Liu, *IEEE Elec. Dev. Lett.*, **23**, 185 (2002).
5. M.Y. Yang, C.H. Huang, A. Chin, C. Zhu, B.J. Cho., M.F. Li, and D. L. Kwong, *IEEE Microwave and Wireless Compo. Lett.*, **13**, 431 (2003).
6. H. Hu, C. Zhu, B.J. Cho, and W.K. Choi, *IEEE Elec. Dev. Lett.*, **23**, 514 (2002).
7. S.J. Kim, B.J. Cho, M.F. Li, X. Yu, C. Zhu, A. Chin, and D.L. Kwong, *IEEE Elec. Dev. Lett.*, **24**, 387 (2003).
8. S.J. Ding, H. Hu, H.F. Lim, S.J. Kim, X.F. Yu, C. Zhu, B.J. Cho, D. S.H. Chan, S.C. Rustagi, M.B. Yu, A. Chin, and D.L. Kwong, *IEEE Elec. Dev. Lett.*, **23730** (2002).
9. H. Hu, C. Zhu, X. Yu, A. Chin, M.F. Li, B.J. Cho, D.L. Kwong, P.D. Foo, M.B. Yu, X. Liu, and J. Winkler, *IEEE Elec. Dev.*, Lett. **24**, 60 (2003).
10. S.J. Ding, H. Hu, C. Zhu, S.J. Kim, X. Yu, M.F. Li, B.J. Cho, D.S.H. Chan, M.B. Yu, S.C. Rustagi, A. Chin, and D.L. kwong, *IEEE Tran. Elec. Devs.*, **51**, 886 (2004).
11. T. Negas, G. Yeager, S. Bell, N. Coats, and I. Minis, *J. Am. Ceram. Soc. Bull.*, **72**, 80 (1993).
12. J.H. Choy, Y.S. Han, J.H. Sohn, and M. Itoh, *J. Am. Ceram. Soc.*, **78**, 1169 (1995).
13. M. Cernea, E. Chirtop, D. Neacsu, I. Pasuk, and S. Iordanescu, *J. Am. Ceram. Soc.*, **85**, 499 (2002).
14. Z. Ma, Z. Becker, A.J. Polakos, P. Huggins, H. Pastalan, J. Wu, H. Watts, K. Wong, Y.H., and Mankiewich, *IEEE Trans. Ele. Dev.*, **45**, 1811 (1998).
15. Y.J. Kim, J. Oh, T.G. Kim, and B.W. Park, *Appl. Phy. Lett.*, **78**, 2363(2001).
16. B.Y. Jang, Y.H. Jeong, S.J. Lee, S. Nahm, H.J. Sun, and H.J. Lee, *J. Eur. Cer. Soc.,* (in press).
17. The International Technology Roadmap for Semiconductors (2004).